

Document downloaded from:

<http://hdl.handle.net/10251/145565>

This paper must be cited as:

Quiles-Carrillo, L.; Montanes, N.; Lagaron, J.; Balart, R.; Torres-Giner, S. (15-0). In Situ Compatibilization of Biopolymer Ternary Blends by Reactive Extrusion with Low-Functionality Epoxy-Based Styrene Acrylic Oligomer. *Journal of Polymers and the Environment*. 27(1):84-96. <https://doi.org/10.1007/s10924-018-1324-2>



The final publication is available at

<https://doi.org/10.1007/s10924-018-1324-2>

Copyright Springer-Verlag

Additional Information

1 ***In Situ* Compatibilization of Biopolymer Ternary Blends with Tunable**
2 **Properties by Reactive Extrusion with Low-functionality Epoxy-based**
3 **Styrene–Acrylic Oligomer**

4 L. Quiles-Carrillo¹, N. Montanes¹, J.M. Lagaron², R. Balart¹, S. Torres-Giner^{1,2*}

5 ¹ *Technological Institute of Materials (ITM), Universitat Politècnica de València (UPV),*
6 *Plaza Ferrándiz y Carbonell 1, Alcoy 03801, Spain*

7 ² *Novel Materials and Nanotechnology Group, Institute of Agrochemistry and Food*
8 *Technology (IATA), Spanish Council for Scientific Research (CSIC), Calle Catedrático*
9 *Agustín Escardino Benlloch 7, Paterna 46980, Spain*

10 * *Corresponding author: storreginer@iata.csic.es and storresginer@upv.es*

11 **Abstract.** The present study originally reports on the use of low-functionality
12 epoxy-based styrene–acrylic oligomer (ESAO) to compatibilize immiscible
13 ternary blends made of poly(3-hydroxybutyrate-*co*-3-hydroxyvalerate) (PHBV),
14 polylactide (PLA), and poly(butylene adipate-*co*-terephthalate) (PBAT). The
15 addition of 2 parts per hundred resin (phr) of low-functionality ESAO during
16 melt processing successfully changed the soften inclusion phase in the blend
17 system to a thinner morphology, yielding biopolymer ternary blends with
18 exceptionally higher mechanical ductility and improved oxygen barrier
19 performance. The compatibilization achieved was ascribed to the *in situ*
20 formation of a newly block terpolymer, *i.e.* PHBV-*b*-PLA-*b*-PBAT, which was
21 produced at the blend interface by the reaction of the multiple epoxy groups
22 present in ESAO with the functional terminal groups of the biopolymers.
23 Additionally, this reaction was mainly linear due to the inherent low
24 functionality of ESAO and the more favorable reactivity of the epoxy groups with
25 the biopolymer carboxyl groups, avoiding the formation of highly branched
26 and/or cross-linked structures and facilitating the films processability. The here-
27 described reactive blending of the selected biopolymers at different mixing ratios
28 represents a suitable industrial methodology to prepare sustainable plastics with
29 tunable properties, excluding any synthesis stage or chemical modification, and
30 of potential application interest in the food packaging field.

31 **Keywords:** PHBV; PLA; PBAT; Reactive extrusion; Sustainable packaging

32 1. INTRODUCTION

33 The future scarcity of petroleum and the strong awareness of post-consumer
34 plastic wastes are the two main drivers behind the interest, at both academic and
35 industrial levels, in biopolymers. The terms “bio-based polymers” and
36 “biodegradable polymers” are extensively used in the polymer literature when
37 referring to biopolymers.^[1] Bio-based polymers include both naturally occurring
38 macromolecules, such as proteins and carbohydrates, or polymers synthesized
39 from renewable monomers. Biodegradable polymers undergo rapidly and
40 completely disintegration through the action of enzymes and/or chemical
41 deterioration associated with living microorganisms. Bio-based polymers can be
42 either non-degradable, such as bio-based polyethylene (bio-PE)^[2] and bio-based
43 polyamides (bio-PAs),^[3] or biodegradable. Among biodegradable polymers, bio-
44 based aliphatic polyesters, including polyhydroxyalkanoates (PHAs) and
45 polylactides (PLAs), play a predominant role due to their potentially
46 hydrolysable ester bonds. Some other biodegradable polyesters can be produced
47 from non-renewable petroleum resources, which is the case of, for instance,
48 poly(butylene succinate) (PBS), poly(butylene succinate-co-adipate) (PBSA), and
49 poly(butylene adipate-co-terephthalate) (PBAT).

50 PHAs are aliphatic polyesters produced by bacterial fermentation with the
51 highest potential to replace polyolefins. PHAs generally consist of 3 to 6
52 hydroxycarboxylic acids and more than 150 monomers have been identified as
53 their constituents.^[4] Such diversity allows the production of biopolymers with a
54 wide range of properties.^[5] Poly(3-hydroxybutyrate) (PHB) homopolymer and
55 its copolymer with 3-hydroxyvalerate (HV), *i.e.* poly(3-hydroxybutyrate-co-3-
56 hydroxyvalerate) (PHBV) are the most important PHAs. The copolymer has
57 lower crystallinity and stiffness while improved flexibility and toughness,
58 broadening both their processing window and applications.^[6] However, most
59 PHA materials cannot be easily processed in current processing equipment and
60 are excessively rigid and brittle for a large number of packaging applications.

61 PLA also belongs to the family of aliphatic polyesters and it is synthetically
62 produced in continuous *via* ring-opening polymerization (ROP) of the lactide
63 dimer.^[7] This monomer is habitually obtained from carbohydrate resources,
64 including agricultural by-products.^[8] Since it contains two chiral carbon centers,
65 PLA can coexist in three stereochemical forms: poly(L-lactide) (PLLA), poly(D-
66 lactide) (PDLA), and poly(DL-lactide) (PDLLA).^[9] Most commercial grades of
67 PLA are indeed copolymers of PLLA and PDLLA,^[10] which can be easily melt
68 processed in conventional processing methodologies, including film and sheet
69 extrusion, injection molding, thermoforming, foaming, and fiber spinning, to
70 produce habitually rigid articles.^[11] However, the major drawbacks of PLA are
71 related to its low heat distortion temperature (HDT) and toughness due to its
72 glass transition temperature ($T_g \sim 60$ °C) and intrinsic brittleness, respectively.
73 Therefore, to overcome these drawbacks, a large research activity is being carried
74 out by melt mixing with both natural fillers^[12] and plasticizers.^[13, 14]

75 PBAT is a semi-aromatic copolyester that is synthetically obtained by
76 polycondensation reaction between 1,4-butanediol and a mixture of adipic acid
77 and terephthalic acid (TPA), mainly derived from petroleum sources. A range
78 from approximately 35 to 55 mol.-% TPA usually offers an optimal compromise
79 between biodegradability and useful properties.^[15] Because of their high
80 flexibility, PBAT copolyesters are mostly interesting for flexible applications (*e.g.*
81 bags and mulch films).^[16] In view of their high toughness, good heat resistance,
82 and high-impact performance, blends of PBAT with other biopolymers, such as
83 PLA,^[17] thermoplastic starch (TPS),^[18] and PBS,^[19] have been studied.

84 Biodegradable polymers are suitable candidates for disposable material
85 applications, particularly in short-term uses, such as packaging and hygiene.
86 However, the use of biopolymers is currently restricted for most industrial
87 applications due to both their poor processability and lower thermal stability and
88 mechanical performance (when taken alone) than commodity polymers. The
89 development of copolymers and biopolymer blends with satisfactory properties
90 can straightforwardly overcome these limitations. In comparison to
91 copolymerization, polymer blends represent an economic and more convenient

92 way to provide the desired properties by physical mixing without any synthesis
93 stage or chemical modification. However, most of the existing polymer blends
94 are not thermodynamically miscible, which is mainly influenced by interactions
95 such as dipole–dipole, ion–dipole, hydrogen bonding, acid–base, and donor and
96 acceptor.^[20, 21] As a result, immiscible polymer blends habitually need to be
97 compatibilized to improve the adhesion between the phase components, reduce
98 their interfacial tension, and generate limited inclusion phase sizes.^[22]

99 Compatibilization in biopolymer blends can be effectively addressed by either *ex*
100 *situ* (non-reactive) or *in situ* (reactive) methods.^[22] *Ex situ* compatibilization is
101 based on the use of a premade (block or grafted) copolymer, being highly
102 miscible with the blend components. However, this is a two-step strategy that is
103 not habitually desirable from an industrial point of view and it is only suitable
104 for specialty polymer systems where the cost of manufacturing and addition of
105 the copolymer is economically feasible.^[23, 24] In addition, it habitually yields a low
106 compatibilizing effect due to it is almost impossible to reach all the added
107 copolymer at the interface of the immiscible blend.^[25-27] Alternatively, *in situ*
108 compatibilization is performed by means of polymers, oligomers, and additives
109 containing multi-functional groups (*e.g.* anhydride, epoxy, oxazoline,
110 isocyanates, etc.). These are capable of reacting during melt processing with the
111 hydroxyl and carboxyl functional groups of condensation polymers.^[28] For this,
112 it is important that the reactive compatibilizers possess low melt viscosity so that
113 they can easily diffuse to the blends interface within a short processing time.^[22]

114 *In situ* compatibilization of biopolymer blends with additives of low-molecular
115 weight (M_w), such as reactive oligomers and oils, is both economically and
116 environmentally more favorable because it involves the use of a relatively low
117 concentration of compatibilizer, typically below 5 wt.-%, in a one-step process.^{[22,}
118 ^{29]} Recent studies have concluded that it results in the formation of *in situ*
119 copolymers that improve drop breakup and stabilize coalescence in the blend
120 systems.^[30, 31] Among the studied reactive compatibilizers, epoxy-based styrene–
121 acrylic oligomers (ESAOs) with different degree of functionalities and a low M_w ,
122 well below 9000 g/mol, can easily form new ester bonds through reaction of their

123 epoxy groups with the terminal functional groups of the biopolymer chains. This
124 mainly consists on glycidyl esterification of carboxylic acid end groups, which
125 precedes hydroxyl end group etherification.^[32] In ESAOs, styrene and acrylate
126 building blocks are each typically 1–20 and 2–20, respectively, having glycidyl
127 and epoxy groups incorporated as side chains.^[33] By the epoxy ring-opening and
128 subsequent reaction with both the hydroxyl and carboxylic acid end groups,
129 ESAOs can efficiently reconnect the polyester chains that break down during
130 melt processing. These additives are habitually termed as “chain extenders”
131 since the M_W of the biopolymers is increased (or recovered if hydrolysis
132 simultaneously occurs).^[34] The resultant biopolymer articles typically present
133 enhanced mechanical performance and thermal stability due to their increased
134 M_W .^[35, 36] Since the melt-processing time is sufficient to accomplish chain
135 reaction, this method presents a great deal of potential for *in situ*
136 compatibilization of polymer blends at industrial scale.^[37]

137 In ESAOs, the average number of epoxy groups per chain habitually lies between
138 4 and 9. This reactive oligomer can form *in situ* block copolymers by the hydrogen
139 abstraction from the carboxyl group of blended polyesters.^[38] However, most
140 tested ESAO grades present high number average functionality (f), typically ~ 9 ,
141 *i.e.* the so-called multi-functional ESAO (Joncryl® ADR 4368-C),^[33] which can
142 easily lead to the formation of highly chain-branched and/or cross-linked
143 structures.^[38] This may result in a dramatic reduction of the melt flow index (MFI)
144 of the blended system, which could both limit its processing (*e.g.* injection
145 molding) and originate gel formation. On the contrary, both bi-functional ESAO,
146 *i.e.* with f values of ~ 2 , and low-functionality ESAO, *i.e.* with f values of 4–5, can
147 raise melt viscosity through linear chain-extension or moderate branching.^[39]

148 The present study reports, for the first time, the use of low-functionality ESAO to
149 *in situ* compatibilize ternary blends of three commercial biodegradable
150 polyesters, namely PHBV, PLA, and PBAT, by reactive extrusion (REX). These
151 biopolymers were selected as they are currently produced in relatively large
152 volumes and present a very dissimilar performance, so their combination can
153 provide tunable properties for a broad packaging application range.

154 2. EXPERIMENTAL

155 2.1. Materials

156 Bacterial aliphatic copolyester PHBV was ENMAT™ Y1000P, produced by
157 Tianan Biologic Materials (Ningbo, China). This biopolymer resin presents a
158 density of 1.23 g/cm³ and a melt flow index (MFI) of 5–10 g/10 min (190 °C, 2.16
159 kg). The HV fraction in the copolyester is 2–3 mol.-%.

160 Homopolyester PLA, grade Ingeo™ biopolymer 2003D, was obtained from
161 NatureWorks (Minnetonka, MN, USA). Density is 1.24 g/cm³ and MFI is ~6 g/10
162 min (210 °C, 2.16 kg). The D-lactide isomer content is 3.8–4.2 wt.-%.

163 Petrochemical copolyester PBAT, termed as Biocosafe 2003F, was purchased
164 from Xinfu Pharmaceutical Co. Ltd. (Zhejiang, China). This resin presents a MFI
165 value of ≤ 5 g/10 min (150 °C, 2.16 Kg) and a density of 1.18–1.28 g/cm³. The
166 butylene adipate (BA)-to-butylene terephthalate (BT) ratio in the copolyester is
167 approximately 55/45 (mol/mol).

168 Low-functionality ESAO was obtained from BASF S.A. (Barcelona, Spain), in the
169 form of solid granules, under the trade name Joncryl® ADR 4300. Its M_w is 5500
170 g/mol, T_g is 56 °C, the epoxy equivalent weight (EEW) is 445 g/mol, and *f* is ≤ 5.
171 Manufacturer recommends a dosage of 0.4–2wt.-% in polyesters.

172 2.2. Melt processing

173 Prior to processing, all biopolymer pellets were dried in an Industrial Marsé
174 MDEO dehumidifier (Barcelona, Spain) at 60 °C for at least 12 h. Drying was
175 necessary to minimize hydrolytic degradation of the biopolyesters.

176 The neat biopolymers and their ternary blends were melt compounded in a co-
177 rotating ZSK-18 MEGAlab laboratory twin-screw extruder from Coperion
178 (Stuttgart, Germany). The screws feature 18 mm diameter with a length (L) to
179 diameter (D) ratio, *i.e.* L/D, of 48. The biopolymer pellets and ESAO granules
180 were manually pre-homogenized in a zipper bag and then fed into the main
181 hopper. The materials dosage was set to achieve a residence time of about 1 min,
182 measured by a blue masterbatch. The extrusion temperature profile, from the

183 hopper to the die, was set as follow: 155, 160, 160, 165, 165, 170, and 175 °C. The
 184 strand was cooled in a water bath at 15 °C and pelletized using an air-knife unit.
 185 Films with a mean thickness of 200–250 µm were obtained by thermo-
 186 compression in a hydraulic press 3850-model from Carver, Inc. (Wabash, IN,
 187 USA). The process was performed at 180 °C and 8 bar for 10 min, followed by
 188 fast cooling inside the press using an internal water system at 15 °C for 5 min.
 189 The films were stored at room conditions, *i.e.* 23 °C and 50% HR, for at least 15
 190 days before characterization.

191 **Table 1** summarizes the composition of the here-prepared biopolymer films.
 192 Addition of low-functionality ESAO was set at a fixed content of 2 parts per
 193 hundred resin (phr) of biopolymer.

194 **Table 1.** Films composition according to the weight content (wt.-%) of poly(3-
 195 hydroxybutyrate-*co*-3-hydroxyvalerate) (PHBV), polylactide (PLA), and
 196 poly(butylene adipate-*co*-terephthalate) (PBAT). Low-functionality epoxy-based
 197 styrene–acrylic oligomer (ESAO) was added as parts per hundred resin (phr) of
 198 biopolymer.

Sample	PHBV (wt.-%)	PLA (wt.-%)	PBAT (wt.-%)	ESAO (phr)
PHBV	100	0	0	0
PLA	0	100	0	0
PBAT	0	0	100	0
PHBV/PLA/PBAT 1:1:1	33.33	33.33	33.33	0
PHBV/PLA/PBAT 1:1:1 + ESAO	33.33	33.33	33.33	2
PHBV/PLA/PBAT 2:1:1 + ESAO	50	25	25	2
PHBV/PLA/PBAT 3:1:1 + ESAO	60	20	20	2

199

200 **2.3. Films characterization**

201 **2.3.1. Morphology**

202 The film cross-sections were observed by field emission scanning electron
203 microscopy (FESEM) in a ZEISS ULTRA 55 from Oxford Instruments (Abingdon,
204 United Kingdom). Film specimens were cryo-fractured by immersion in liquid
205 nitrogen and then mounted on aluminum stubs perpendicularly to their surface.
206 The working distance (WD) varied in the 6–7 mm range and an extra high tension
207 (EHT) of 2 kV was applied to the electron beam. Due to their non-conducting
208 nature, samples were subjected to a sputtering process with a gold-palladium
209 alloy in a sputter coater EMITECH-SC7620 from Quorum Technologies, Ltd.
210 (East Sussex, United Kingdom). The sizes of the inclusion phase were determined
211 using Image J Launcher v 1.41 and the data presented were based on
212 measurements from a minimum of 20 SEM micrographs per sample.

213 **2.3.2. Infrared Spectroscopy**

214 Chemical analyses on the film surfaces were performed using attenuated total
215 reflection–Fourier transform infrared (ATR-FTIR) spectroscopy. Spectra were
216 recorded with a Vector 22 from Bruker S.A. (Madrid, Spain) coupling a PIKE
217 MIRacle™ ATR accessory from PIKE Technologies (Madison, USA). Ten scans
218 were averaged from 4000 to 400 cm^{-1} at a resolution of 4 cm^{-1} .

219 **2.3.3. Thermal analysis**

220 Main thermal transitions of the biopolymer films were obtained by differential
221 scanning calorimetry (DSC) in a Mettler-Toledo 821 calorimeter (Schwerzenbach,
222 Switzerland). An average sample weight ranging from 5 to 7 mg was subjected
223 to a heating program from 30 °C to 200 °C at a heating rate of 10 °C min^{-1} in
224 nitrogen atmosphere (66 mL min^{-1}). Standard sealed aluminum crucibles of a
225 volume capacity of 40 μl were used. DSC runs were performed in triplicate.

226 Thermal stability was determined by thermogravimetric analysis (TGA) in a
227 Mettler-Toledo TGA/SDTA 851 thermobalance. Samples, with an average
228 weight between 5 and 7 mg, were placed in standard alumina crucibles of 70 μl

229 and subjected to a heating program from 30 °C to 700 °C at a heating rate of 20 °C
230 min⁻¹ in air atmosphere. TGA experiments were performed in triplicate.

231 **2.3.4. Thermomechanical tests**

232 Dynamic mechanical thermal analysis (DMTA) was conducted in a DMA-1
233 model from Mettler-Toledo, working in tension mode, single cantilever. Film
234 samples sizing 10 × 5 × 0.2 mm³ were subjected to a temperature sweep program
235 from -40 °C to 130 °C at a heating rate of 2 °C min⁻¹, an offset strength of 1N, an
236 offset deformation of 150%, and a control deformation of 6 μm. DMTA tests were
237 run in triplicate.

238 **2.3.5. Mechanical tests**

239 Tensile tests of films were carried out by analyzing standard samples (type-2), as
240 indicated in ISO 527-3, with a total length and width of 160 mm and 10 mm,
241 respectively. The tests were performed in a universal testing machine ELIB 30
242 from S.A.E. Ibertest (Madrid, Spain), equipped with a 5-kN load cell, and using
243 specific pneumatic clamps at a cross-head speed of 5 mm min⁻¹. At least six
244 specimens per sample were tested.

245 **2.3.6. Permeability tests**

246 The water vapor permeability (WVP) was determined according to the ASTM
247 2011 gravimetric method. For this, 5 mL of distilled water were poured into a
248 Payne permeability cup (∅ = 3.5 cm) from Elcometer Sprl (Hermalle-sous-
249 Argenteau, Belgium). The films were placed in the cups so that on one side they
250 were exposed to 100% relative humidity (RH), avoiding direct film contact with
251 water. The cups containing the films were then secured with silicon rings and
252 stored in a desiccator at 25 °C and 0% RH. Identical cups with aluminum foils
253 were used as control samples to estimate water loss through the sealing. The cups
254 were weighed periodically using an analytical balance with ±0.0001 g accuracy.
255 Water vapor permeation rate (WVPR), also called water permeance when
256 corrected for permeant partial pressure, was determined from the steady-state
257 permeation slope obtained from the regression analysis of weight loss data per
258 unit area *vs.* time, in which the weight loss was calculated as the total cell loss

259 minus the loss through the sealing. WVP was obtained, in triplicate, by correcting
260 the permeance by the average film thicknesses.

261 Limonene permeability (LP) was also determined according to ASTM 2011
262 gravimetric method. Similarly, 5 mL of D-limonene, obtained from Sigma-Aldrich
263 S.A. (Madrid, Spain) with 98% purity, was placed inside the Payne permeability
264 cups and the cups containing the films were stored under controlled conditions,
265 *i.e.* 25 °C and 40% RH. Limonene permeation rate (LPR) was obtained from the
266 steady-state permeation slopes. The weight loss was calculated as the total cell
267 loss minus the loss through the sealing plus the water sorption gained from the
268 environment measured in samples with no permeant. LP was calculated taking
269 into account the average sheet thickness in each case, measuring three replicates
270 per sample.

271 Oxygen permeability (OP) was obtained from the oxygen transmission rate
272 (OTR) measurements using an Oxygen Permeation Analyzer M8001 from
273 Systech Illinois (Thame, UK). The samples were previously purged with nitrogen
274 in the humidity equilibrated samples and then exposed to an oxygen flow of 10
275 mL min⁻¹. The exposure area during the test was 5 cm². Test were performed at
276 25 °C and 60% RH and recorded in duplicate.

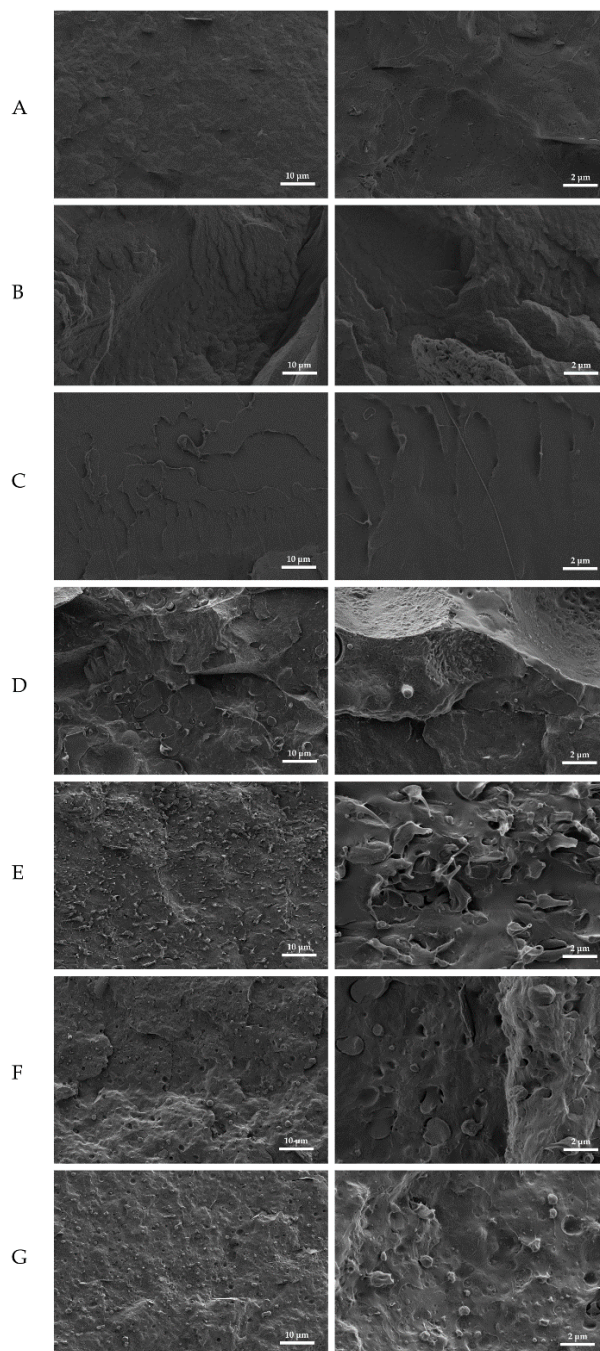
277 3. RESULTS AND DISCUSSION

278 3.1. Morphology

279 **Figure 1** shows the FESEM images, taken at low (left) and high (right)
280 magnification, of the biopolymer film cross-sections obtained by cryo-fracture.
281 As it can be seen in **Figures 1a-c**, all neat biopolymer films presented a relatively
282 homogenous fracture surface with different degrees of roughness. In the case of
283 PHBV and PLA, respectively shown in **Figure 1a** and **1b**, one can also observe
284 that both biopolymer films followed a similar pattern of breakage, showing a
285 rough surface that is representative of brittle materials. This was more noticeable
286 for the PLA film where several micro-cracks were also formed during the

287 fracture. On the contrary, as seen in **Figure 1c**, the PBAT film showed a softer
288 surface, evidencing certain plastic deformation by the presence of long filaments.

289 In relation to the biopolymer blends, gathered in **Figures 1d-g**, these exhibited
290 heterogeneous surfaces that were based on an “island-and-sea” morphology in
291 which a part of each phase was dispersed as small droplets in the others. The
292 absence of a co-continues phase morphology in the blends supports previous
293 studies indicating that, at the here-studied mixing ratios, these biopolymers are
294 thermodynamically immiscible.^[40] However, the droplet sizes of the embedded
295 inclusion phases were considerably larger in the ternary blend film processed
296 without ESAO, in the range of 2–10 μm , as it can be seen in **Figure 1d**. This
297 indicates a rapid coalescence and also a poor interface adhesion between the
298 biopolymer phases. In the case of the ternary blend films melt processed with
299 low-functionality ESAO, the inclusion phases were stretched into submicron
300 droplets, *i.e.* lower than 1 μm , indicating that a higher coalescence stabilization
301 of the biopolymer phases was achieved. As seen in **Figure 1g**, for the ternary
302 blend film melt processed with ESAO and with the highest PHBV content, *i.e.* 80
303 wt.-%, the droplets size achieved the lowest value, presenting a mean diameter
304 of approximately 600 nm. This morphological change can be attributed to the
305 achievement of a partial miscibility in the biopolymer ternary blends that, as one
306 can expect, increased as the PHBV content was higher. A similar effect of ESAO
307 was observed, for instance, by Ojijo *et al.*^[38] on PLA/PBSA blends, in which the
308 inclusion phase size was significantly reduced from 2.69 to 0.7 μm due to a
309 reduced surface tension between the phases. A previous study consisting of PLA
310 and PBAT blends compatibilized using ESAO also suggested that partial
311 miscibility is achieved through the *in situ* formation of a block copolymer ^[41].



312

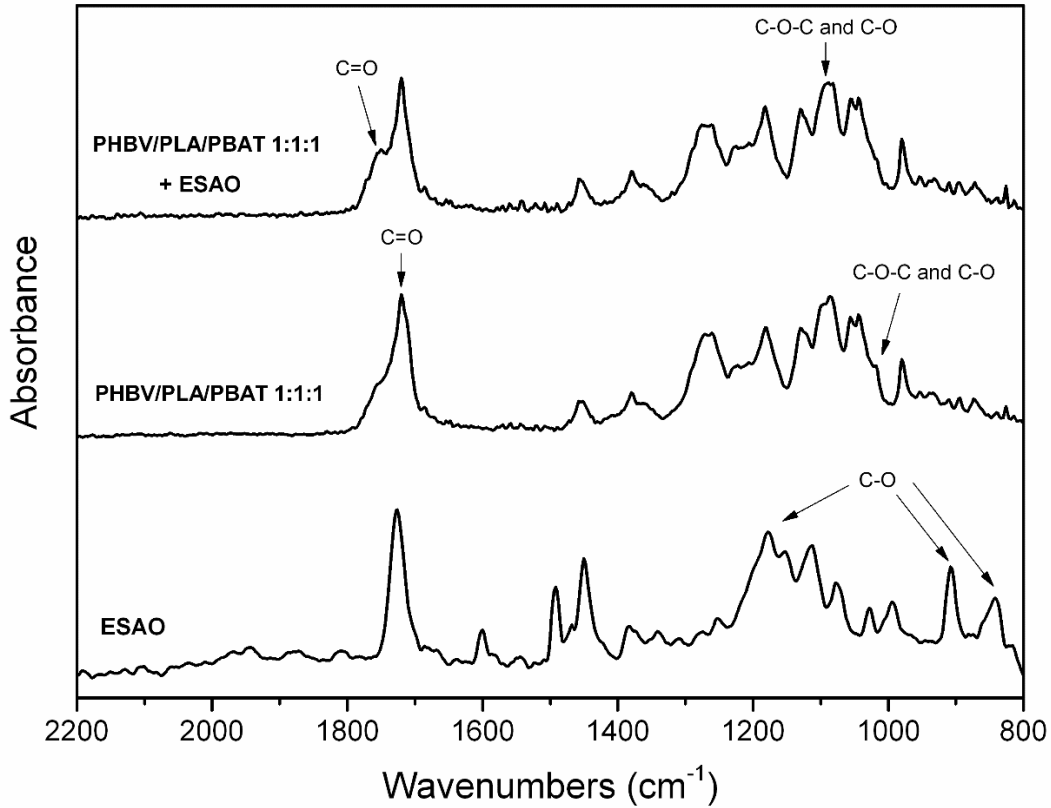
313 **Figure 1.** Field emission scanning electron microscopy (FESEM) images of the
 314 cryofracture surfaces taken at 1000x (left) and 5000x (right) corresponding to the
 315 films made of: a) Poly(3-hydroxybutyrate-co-3-hydroxyvalerate) (PHBV); b)
 316 Polylactide (PLA); c) Poly(butylene adipate-co-terephthalate) (PBAT); d)
 317 PHBV/PLA/PBAT 1:1:1; e) PHBV/PLA/PBAT 1:1:1 with low-functionality
 318 epoxy-based styrene-acrylic oligomer (ESAO); f) PHBV/PLA/PBAT 2:1:1 with
 319 ESAO; g) PHBV/PLA/PBAT 3:1:1 with ESAO.

320 One can additionally observe that, after melt processing the ternary blends with
321 ESAO, the fracture surface behavior of their films predominantly changed from
322 brittle to ductile. In the case of the uncompatibilized blend film, *i.e.* the ternary
323 blend melt processed without ESAO, it presented a clear pull-out of the inclusion
324 phase after fracture, which is supported by the presence of large holes in **Figure**
325 **1d**. However, the submicron droplets in the ternary blend films processed with
326 ESAO induced a notable plastic deformation with no evidence of phase
327 separation. Therefore, the addition of low-functionality ESAO also improved the
328 adhesion between the blended components, facilitating a better stress transfer
329 from one phase to another phase. In this sense, Lin *et al.*^[42] also reported a
330 significant adhesion improvement in PLA/PBAT blends by means of tetrabutyl
331 titanate (TBT), which decreased the interface between the two biopolymers.
332 Indeed, the resulting biopolymer binary blends only acquired improved
333 performance when the stress transfer between the two blended components was
334 effective. In another work, Arruda *et al.* ^[43] studied the morphology both in
335 machine direction (MD) and transverse direction (TD) of a blown film made of
336 PLA/PBAT processed with and without multi-functional ESAO. The
337 incorporation of ESAO into the blend changed the PBAT inclusion phase shape,
338 in both MD and TD, from platelet to refined fibrillar structure. This morphological
339 change was attributed to the improved compatibility between the phases due to
340 a PLA-*b*-PBAT copolymer formation at the interface of both biopolymers.

341 **3.2. Chemical properties**

342 FTIR was carried out in order to ascertain the chemical interactions of the
343 biopolymer phases after the addition of low-functionality ESAO. **Figure 2** shows
344 the FTIR spectra of the ESAO granules and the films of the ternary blend
345 PHBV/PLA/PBAT 1:1:1 melt-processed with and without low-functionality
346 ESAO. In relation to the ESAO spectrum, the main peaks related to C-O
347 stretching vibration of the epoxy groups appeared at $\sim 1180, 910, \text{ and } 840 \text{ cm}^{-1}$.^{[33,}
348 ^{44-46]} These peaks were not observed in the spectrum of the ternary blend
349 processed with low-functionality ESAO, indicating that the functional groups of
350 the oligomer reacted and were consumed during melt compounding. In this

351 sense, the ESAO reaction in a binary PLA/PBSA blend was previously confirmed
352 by FTIR spectroscopy as a result of the disappearance of the epoxy group bands
353 at 907 and 843 cm^{-1} .^[38]



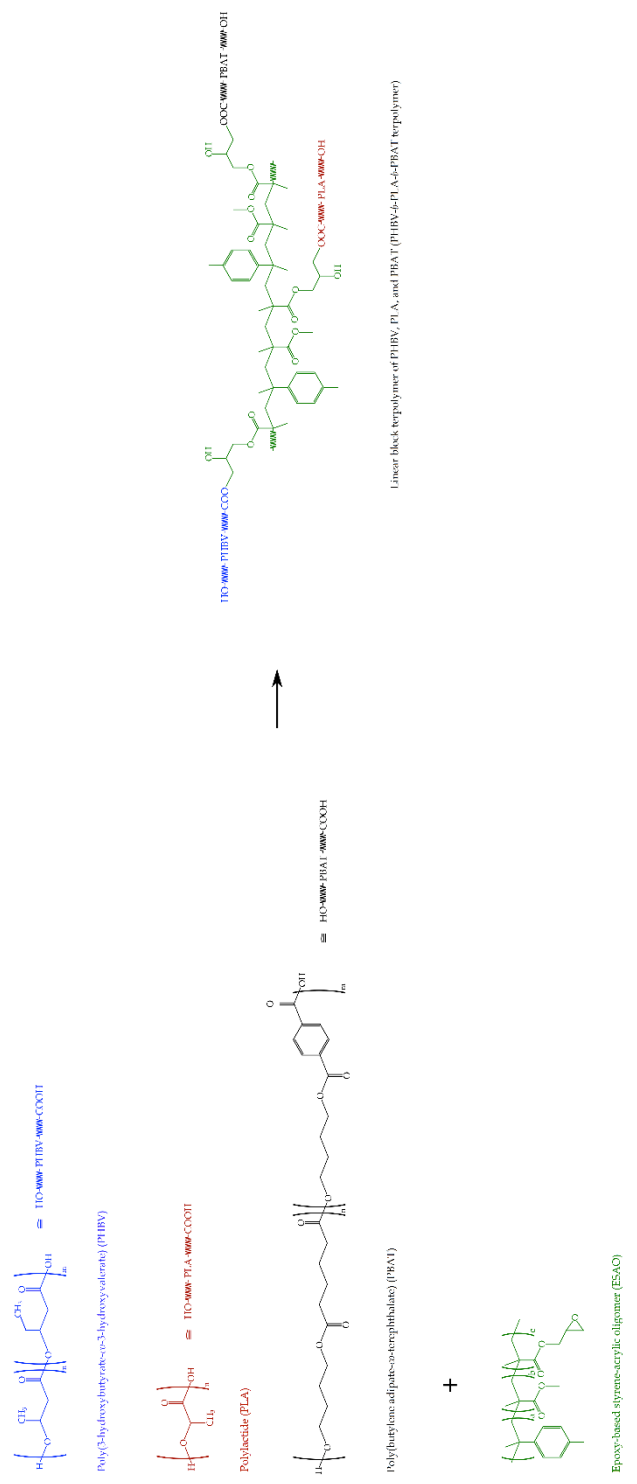
354

355 **Figure 2.** Fourier transform infrared (FTIR) spectra, from bottom to top, of: low-
356 functionality epoxy-based styrene-acrylic oligomer (ESAO) and the ternary
357 blends of poly(3-hydroxybutyrate-co-3-hydroxyvalerate) (PHBV), polylactide
358 (PLA), and poly(butylene adipate-co-terephthalate) (PBAT) processed with and
359 without ESAO. Arrows indicate the chemical bonds described in the text.

360 In relation to the spectra of the biopolymer blends one can observe that the
361 strongest band of the polyesters, attributed to their C=O stretching ^[12], slightly
362 broadened and shifted from 1721 cm^{-1} , for the uncompatibilized ternary blend,
363 to 1718 cm^{-1} , for the ternary blend melt processed with ESAO. The shoulder of
364 the carbonyl peak centered at $\sim 1750 \text{ cm}^{-1}$ also became more intense in the
365 compatibilized film. A similar peak change was previously ascribed to the
366 reaction between the epoxy groups of multi-functional ESAO and the carboxyl

367 groups (-COO) in polyesters.^[47] This observation has been also related to a
368 disruption of the hydrogen bonding in the molecular arrangement of the PHA
369 chains,^[33] which further supports the presence of a newly formed copolyester. It
370 is also worthy to mention the slight increase observed for the ester-related band
371 at $\sim 1080\text{ cm}^{-1}$ that was accompanied to the reduction of the band at $\sim 1020\text{ cm}^{-1}$,
372 which are known to arise from C-O and C-O-C stretching vibrations of ester
373 groups in biopolyesters.^[48] Though these changes were subtle, they may suggest
374 a reduction of the former ester bonds in the biopolymers as well as the formation
375 of new ones.

376 According to the above-described chemical interactions, **Figure 3** proposes the
377 chemical reaction of the three biopolymers with the epoxy functional groups of
378 low-functionality ESAO during melt processing. The proposed scheme suggests
379 the formation of a new copolyester, which first involves the ring-opening of
380 epoxy groups in ESAO and their subsequent reaction with the carboxyl groups
381 of the terminal acids of the biopolymers to create new covalent C-O-C bonds.
382 This chain-linking process is considered to be mainly linear based on the fact that,
383 on the one hand, the reaction rate between epoxy groups with the carboxyl
384 groups in polyesters is about 10-15 times more favorable than with the hydroxyl
385 groups^[41] and, on the other, the here-selected ESAO inherently presents a low
386 functionality. As a result, a linear block terpolymer consisting of PHBV, PLA, and
387 PBAT chains, *i.e.* a PHBV-*b*-PLA-*b*-PBAT terpolymer, and the copolymers based
388 on binary combinations of thereof are proposed to be formed.

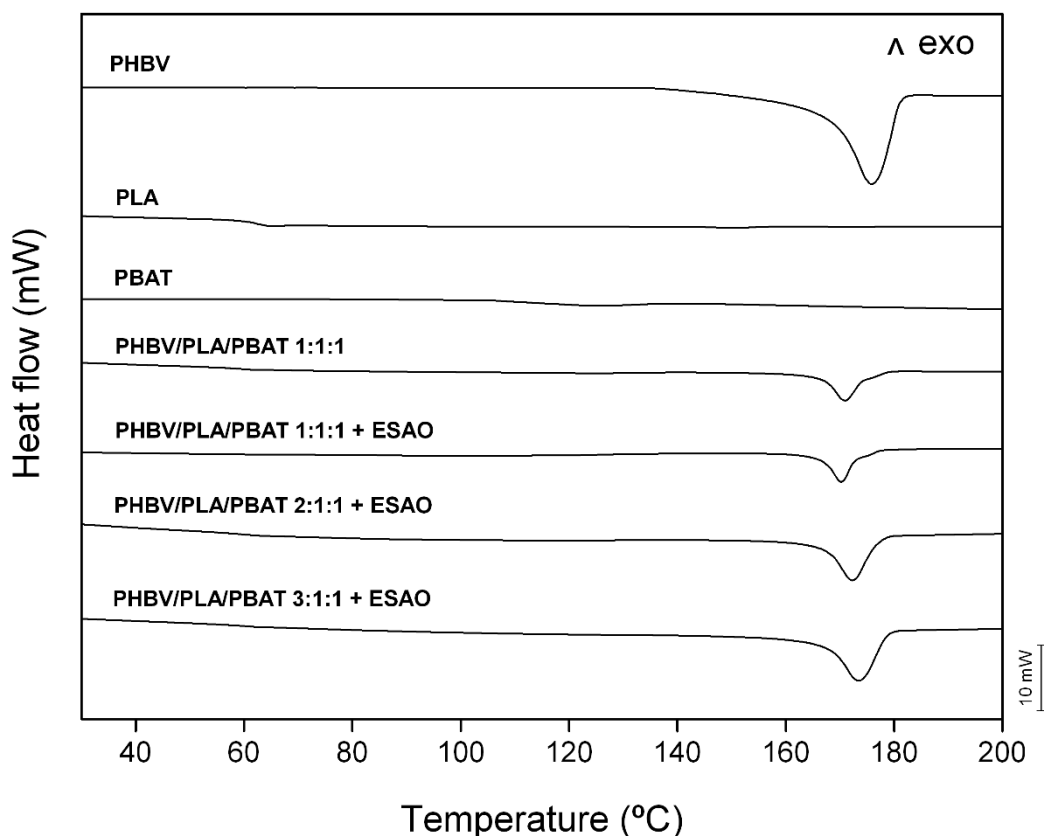


389

390 **Figure 3.** Schematic representation of the *in situ* formed block terpolymer of
 391 poly(3-hydroxybutyrate-*co*-3-hydroxyvalerate) (PHBV), polylactide (PLA), and
 392 poly(butylene adipate-*co*-terephthalate) (PBAT) by low-functionality epoxy-
 393 based styrene-acrylic oligomer (ESAO). An average functionality (*f*) value of 3
 394 was considered for the proposed reaction.

395 3.3. Thermal properties

396 **Figure 4** shows the DSC heating thermograms of the biopolymer films. One can
397 observe that the neat PHBV film presented a sharp melting peak at ~ 175 °C,
398 showing no evidences of cold crystallization during heating. For both PLA and
399 PBAT, the curves showed a slight and poorly defined endothermic peak centered
400 at 151 °C and 124 °C, respectively. This observation suggests that the neat PLA
401 and PBAT films were predominantly amorphous. Since the crystallization
402 behavior is closely related to the biopolymers thermal history, it is considered
403 that PLA and PBAT developed an amorphous structure at the cooling rate of the
404 films. In this sense, Miyata and Masuko^[49] studied the non-isothermal
405 crystallization of PLLA materials at various cooling rates, observing that samples
406 cooled at rates greater than 10 °C min^{-1} did not crystallize and remained
407 amorphous. In the case of the PLA film, a glass transition phenomenon can be
408 seen at ~ 62 °C. This second thermal transition was not observed for the other
409 biopolymer films as it is known to occur under ambient temperature, *i.e.* T_g
410 ranges from -40 °C to 5 °C for PHAs^[5] while it is around -20 °C for PBAT.^[19, 50]
411 In relation to the biopolymer ternary blend films, the DSC curves presented a
412 low-intense glass transition in the 55 – 65 °C range and a melting process in the
413 temperature range of 165 – 180 °C corresponding to the PLA and PHBV phases,
414 respectively. Additionally, it can be observed that the T_m values gradually
415 increased with increasing the PHBV content, ranging from ~ 171 °C, for the 1:1:1
416 blends, to 174 °C, for the 3:1:1 blend. The melting enthalpies were also higher in
417 the blend films with higher PHBV content.

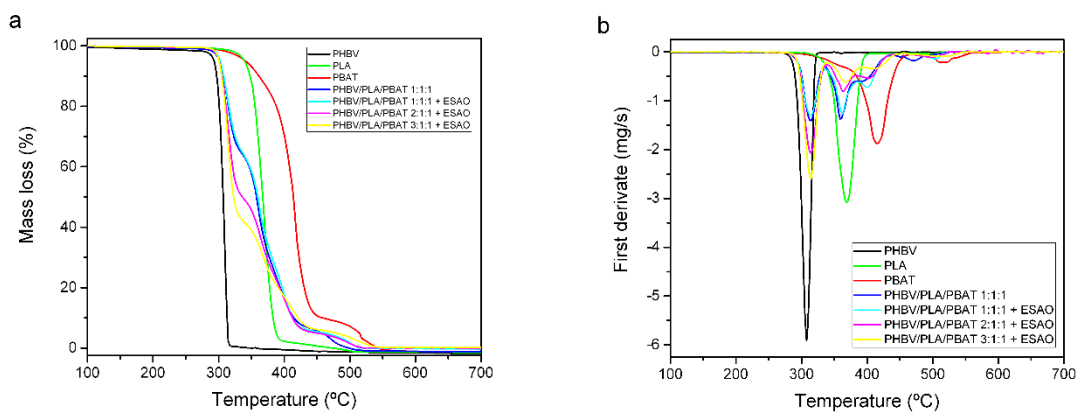


418

419 **Figure 4.** Differential scanning calorimetry (DSC) thermograms of the ternary
 420 blend films made of poly(3-hydroxybutyrate-*co*-3-hydroxyvalerate) (PHBV),
 421 polylactide (PLA), and poly(butylene adipate-*co*-terephthalate) (PBAT)
 422 processed with and without low-functionality epoxy-based styrene-acrylic
 423 oligomer (ESAO).

424 **Figure 5** includes both the TGA curves, in **Figure 5a**, and their corresponding
 425 derivative thermogravimetric (DTG) curves, in **Figure 5b**, of the biopolymer
 426 films in the 100–700 °C range. One can clearly observe that PHBV presented the
 427 lowest thermal stability, fully decomposing in a sharp single step. The values of
 428 onset degradation temperature, determined as the degradation temperature at
 429 5% of mass loss ($T_{5\%}$), and degradation temperature (T_{deg}) were ~ 294 °C and 310
 430 °C, respectively. On the contrary, both PLA and PBAT, particularly the latter,
 431 presented a relatively high thermal stability, showing $T_{5\%}$ values around 340 °C.
 432 Both biopolymers decomposed in two stages with T_{deg} values at approximately

433 390 °C and 480 °C, for PLA, and 430 °C and 510 °C, for PBAT. All ternary blends
 434 showed a thermal stability profile relatively close to that of neat PHBV, though
 435 the onset was slightly delayed up to ~300 °C. It is also worthy to mention that the
 436 thermal decomposition of the blends took place in three different stages, in which
 437 the second mass loss, which was observed in the 325–375 °C range, is mainly
 438 related to the PHBV phase. Therefore, the effect of the low-functionality ESAO
 439 addition on the thermal behavior and stability of the blends was relatively low,
 440 whereas PHBV played the major role in their thermal degradation.



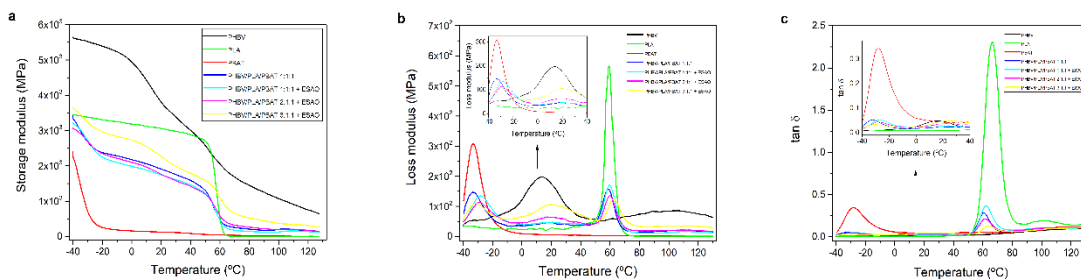
441

442 **Figure 5.** a) Thermogravimetric analysis (TGA) and b) derivative
 443 thermogravimetric (DTG) curves of the ternary blend films made of poly(3-
 444 hydroxybutyrate-*co*-3-hydroxyvalerate) (PHBV), polylactide (PLA), and
 445 poly(butylene adipate-*co*-terephthalate) (PBAT) processed with and without
 446 low-functionality epoxy-based styrene–acrylic oligomer (ESAO).

447 3.4. Thermomechanical properties

448 In order to fully determine the T_g of the biopolymer blends and also to further
 449 ascertain the potential effect of low-functionality ESAO on their miscibility,
 450 DMTA was carried out from -40 °C to 130 °C. The evolution of the storage
 451 modulus, loss modulus, and damping factor ($\tan \delta$) *vs.* temperature of the
 452 biopolymer films are included in **Figure 6**. The storage modulus is a measure of
 453 the energy stored and recovered in a cyclic deformation and it represents the
 454 stiffness of the films. As shown in **Figure 6a**, at -40 °C, the neat PHBV film

455 showed a value around 5600 MPa. This was significantly higher than those of
 456 PLA and PBAT, which then resulted in more flexible films, having values of 3450
 457 MPa and 2400 MPa, respectively. The storage modulus of PHBV started to
 458 decrease at approximately 0 °C, which corresponds to the initiation of alpha (α)-
 459 transition region of this biopolymer. In the case of the PLA film, this
 460 thermomechanical change was observed at \sim 55 °C, while for the PBAT film this
 461 overlapped with the beginning of the measurement, *i.e.* -40 °C. In addition, the
 462 softening of the PLA and PBAT films with increasing temperature was also more
 463 intense. This confirms that a higher fraction of the biopolymer molecules
 464 underwent glass transition, as previously observed by DSC analysis. Similar
 465 DMTA curves were reported for PLA and PBAT binary blends by Abdelwahab
 466 *et al.* [46], who also revealed that the addition of 1 phr ESAO increased the storage
 467 modulus for samples containing lignin. In the present study, all biopolymer
 468 blend films presented intermediate values of storage modulus, which increased
 469 as the PHBV content was increased. Comparison of the ternary blend with and
 470 without low-functionality ESAO indicated that the addition of this reactive
 471 additive slightly reduced the storage modulus, *i.e.* the film samples became more
 472 flexible. This effect was especially notable at low temperatures, indicating that
 473 this reactive oligomer acted as a plasticizer.



474

475 **Figure 6.** Dynamic mechanical thermal analysis (DMTA) curves of the ternary
 476 blend films made of poly(3-hydroxybutyrate-co-3-hydroxyvalerate) (PHBV),
 477 polylactide (PLA), and poly(butylene adipate-co-terephthalate) (PBAT)
 478 processed with and without low-functionality epoxy-based styrene-acrylic
 479 oligomer (ESAO).

480 The evolution of loss modulus *vs.* temperature is depicted in **Figure 6b**. These
481 curves showed a sharp peak during the α -transition, which is related to the
482 biopolymers T_g s and it is proportional to the energy increase that is dissipated in
483 the films during the loading cycle. This further confirms that each biopolymer
484 undergoes its glass-rubber transition at very different temperatures. The
485 maximum values of loss modulus were particularly observed at approximately -
486 34 °C (0.31 GPa), 13 °C (0.2 GPa), and 58 °C (0.56 GPa) for PBAT, PHBV, and PLA,
487 respectively. In the case of the uncompatibilized blend, this film sample
488 presented three α -peaks related to each biopolymer phase, at temperatures very
489 similar to the ones observed for the neat biopolymers. Interestingly, the ternary
490 blends compatibilized with low-functionality ESAO presented a clear shift of α -
491 peaks to intermediate temperatures of the blended biopolymers. For instance, the
492 α -peak related to the PBAT phase of the 1:1:1 blend moved to -34 °C (0.31 GPa),
493 *i.e.* an increase of 4.5 °C. Similarly, for ternary blend films with higher contents
494 of this biopolymer, the α -peak related to the PHBV increased to values in the 19
495 °C range. Indeed, the study of T_g , in addition to morphology, can be efficiently
496 used to differentiate the level of miscibility in polymer blends. Whereas
497 thermodynamically immiscible blends show different distinguishable T_g values,
498 blends made of two polymers that constitute a completely miscible blend present
499 a single T_g and partially miscible blends have tendency to shift the T_g value of the
500 one component toward that of the other. The here-observed shifts of T_g thus
501 support the partial miscibility of the ternary blends. Similarly, Ren *et al.*^[51] also
502 observed a slight T_g decrease in binary and ternary blends of TPS, PLA, and
503 PBAT with increasing contents of the latter biopolymer.

504 Analogous observations were further found in **Figure 6c** for the damping factor,
505 which relates the ratio of the energy lost to the energy stored in a cyclic
506 deformation. However, the peak displacements related to state changes in the
507 films presented a lower intensity than in the case of the loss modulus. It is also
508 worthy to note the observed enhancement in the $\tan \delta$ peak with the addition of
509 low-functionality ESAO. For instance, at 60 °C, it increased from a value of 0.275,
510 for the uncompatibilized blend, up to a value of 0.36, in the case of compatibilized

511 blend, *i.e.* an improvement close to 30%. This directly implies a greater energy
512 dissipation and improved toughness for the ternary blends processed with low-
513 functionality ESAO.

514 **3.5. Mechanical properties of ternary blends**

515 **Table 2** summarizes the tensile properties of the neat biopolymers and their
516 ternary blends. One can observe that both PHBV and PLA biopolymers produced
517 rigid films with relatively high modulus (E), *i.e.* 800–1200 MPa, and tensile
518 strength (σ_y), *i.e.* 30–40 MPa. As a result, both biopolymers share some
519 mechanical similarities with traditional rigid polymers, such as polyethylene
520 terephthalate (PET), polystyrene (PS), polypropylene (PP), and polycarbonate
521 (PC), making them as an attractive alternative for disposable and compostable
522 rigid articles.^[52, 53] However, these films were also very brittle, presenting values
523 of elongation at break (ϵ_b) lower than 6%, which limits their application in flexible
524 packaging. In contrast, the PBAT film was very flexible and ductile, reaching ϵ_b
525 values of ~900%. In this sense, it has been reported that PBAT has mechanical
526 properties similar to that of low-density polyethylene (LDPE).^[54]

527 Melt blending of the three biopolymers without ESAO compatibilizer resulted in
528 a film with intermediate mechanical strength values but still with poor ductility.
529 Due to insufficient adhesion between the different phases, it is considered that
530 the soft PBAT domains acted as stress concentrators because of the different
531 elasticity, favoring mechanical failure during the tensile test. A similar effect was
532 recently observed for uncompatibilized PLA/PBAT/PBS blends, in which the
533 stress concentration resulted in a high triaxial stress in the PBAT domain that
534 provoked debonding at the particle–matrix interface.^[55] This observation
535 correlates well with the FESEM images shown above. Interestingly, the same
536 ternary biopolymer blend melt processed with low-functionality ESAO
537 presented higher mechanical values but with an extraordinary improvement in
538 ductility. In particular, if the PHBV/PLA/PBAT 1:1:1 blend is compared to the
539 neat PHBV film, E and σ_y values were improved by more than 10% and 35%,
540 respectively, while ϵ_b value was almost 8 times higher. For the whole studied

541 composition range, higher contents of PHBV in the ternary blends gradually
 542 provided greater mechanical strength properties but also lower ductility.
 543 Therefore, the preparation of different mixing ratios remarkably resulted in
 544 biopolymer films with tunable mechanical properties.

545 **Table 2.** Mechanical properties of the films made of poly(3-hydroxybutyrate-*co*-
 546 3-hydroxyvalerate) (PHBV), polylactide (PLA), and poly(butylene adipate-*co*-
 547 terephthalate) (PBAT) processed with and without low-functionality epoxy-
 548 based styrene-acrylic oligomer (ESAO) in terms of elastic modulus (E), tensile
 549 strength at yield (σ_y), and elongation at break (ϵ_b).

Sample	E (MPa)	σ_y (MPa)	ϵ_b (%)
PHBV	1151.2 ± 63.8	30.4 ± 1.2	2.1 ± 0.1
PLA	822.5 ± 18.3	39.6 ± 1.3	5.5 ± 0.3
PBAT	42.6 ± 1.5	11.6 ± 0.5	901.2 ± 39.6
PHBV/PLA/PBAT 1:1:1	583.1 ± 17.4	14.1 ± 0.9	4.4 ± 0.2
PHBV/PLA/PBAT 1:1:1 + ESAO	644.8 ± 29.6	19.1 ± 0.7	35.1 ± 1.6
PHBV/PLA/PBAT 2:1:1 + ESAO	756.8 ± 28.3	20.2 ± 0.8	7.2 ± 0.5
PHBV/PLA/PBAT 3:1:1 + ESAO	788.6 ± 23.7	21.0 ± 0.9	4.6 ± 0.3

550

551 The here-observed mechanical improvement is in agreement with some previous
 552 works related to biopolymer blends obtained by REX. For instance, addition of
 553 either 2 or 5 wt.-% of glycidyl methacrylate (GMA) during melt compounding to
 554 an immiscible PLA/PBAT binary blend resulted in an increase of the tensile
 555 toughness of the binary blend without severe loss in tensile strength.^[56] In
 556 another work, Ojijo *et al.*^[38] also reported that the elongation at break and impact
 557 strength of compression-molded PLA/PBSA 3:2 blend sheets improved from *ca.*

558 100% to 200% and from 9.8 to 34.7 kJ/m², respectively, with the incorporation of
559 1 phr multi-functional ESAO. More importantly, the blends also presented a
560 relatively high tensile strength while simultaneously exhibiting improved
561 thermal stability and favorable crystallinity. More recently, blown PLA/PBAT
562 8:2 films prepared by reactive blending with 1 phr multi-functional ESAO
563 showed a remarkably high ϵ_b value of ~250% in comparison to the very low ϵ_b
564 value of 4% of the neat PLA film.^[57] Those binary blend films also possessed high
565 E and σ_y values, *i.e.* 2 GPa and 50–60 MPa, respectively. However, in these
566 previous studies the use of multi-functional ESAO also resulted in a high increase
567 of the melt viscosity, which could limit the industrial applicability of the
568 biopolymer blends.

569 **3.6. Barrier properties of ternary blends**

570 **Table 3** shows the barrier properties in terms of WPV, LP, and OP for the here-
571 developed biopolymer films. The barrier performance is, indeed, one of the main
572 parameters of application interest in the food packaging field. Whereas both
573 water vapor and oxygen barrier properties are important to avoid physical and
574 chemical deterioration, limonene transport properties are usually used as a
575 standard system to test aroma barrier. In the case of the neat biopolymers, one
576 can observe that the PHBV film presented the highest barrier performance in
577 relation to both water vapor and oxygen, showing WVP and OP values of
578 approximately $1.8 \times 10^{-15} \text{ kg m m}^{-2} \cdot \text{Pa}^{-1} \cdot \text{s}^{-1}$ and $2 \times 10^{-19} \text{ m}^3 \text{ m m}^{-2} \cdot \text{Pa}^{-1} \cdot \text{s}^{-1}$,
579 respectively. The PLA film showed the lowest LP value and intermediate values
580 of WVP and OP, while the permeability values of the PBAT film were the highest.
581 In this sense, it has been reported that the water vapor barrier of PLA films is
582 lower than PS but still in the range of PET.^[58] Similarly, it has been reported that
583 the oxygen barrier property of PBAT is around 50% lower than LDPE ^[54], which
584 is already a low barrier material to oxygen. In the case of limonene, as opposed
585 to moisture, this is a strong plasticizing component for PHAs and, then, solubility
586 plays a key role in permeability. For instance, solvent-cast films of PHBV with 12
587 mol.-% HV have been reported to uptake up to 12.7 wt.-% limonene, reaching a
588 LP value of $\sim 2 \times 10^{-13} \text{ kg m m}^{-2} \cdot \text{Pa}^{-1} \cdot \text{s}^{-1}$.^[59] The here-obtained PHBV film was

589 around 20 times more barrier to limonene, which can be ascribed to both the
 590 preparation methodology and its lower HV content.

591 **Table 3.** Barrier properties of the films made of poly(3-hydroxybutyrate-co-3-
 592 hydroxyvalerate) (PHBV), polylactide (PLA), and poly(butylene adipate-co-
 593 terephthalate) (PBAT) processed with and without low-functionality epoxy-
 594 based styrene-acrylic oligomer (ESAO) in terms of water vapor permeability
 595 (WVP), limonene permeability (LP), and oxygen permeability (OP).

Sample	WVP x 10 ¹⁵ (kg · m · m ⁻² · Pa ⁻¹ · s ⁻¹)	LP x 10 ¹⁵ (kg · m · m ⁻² · Pa ⁻¹ · s ⁻¹)	OP x 10 ¹⁸ (m ³ · m · m ⁻² · Pa ⁻¹ · s ⁻¹)
PHBV	1.82 ± 0.37	10.26 ± 0.57	0.21 ± 0.03
PLA	12.31 ± 0.98	3.30 ± 0.41	2.22 ± 0.24
PBAT	33.13 ± 1.46	72.58 ± 3.07	9.14 ± 0.86
PHBV/PLA/PBAT 1:1:1	5.11 ± 0.67	3.14 ± 0.82	1.31 ± 0.14
PHBV/PLA/PBAT 1:1:1 + ESAO	5.86 ± 0.29	3.73 ± 0.79	0.49 ± 0.03
PHBV/PLA/PBAT 2:1:1 + ESAO	4.78 ± 0.79	4.34 ± 0.37	0.35 ± 0.19
PHBV/PLA/PBAT 3:1:1 + ESAO	2.75 ± 0.68	4.99 ± 0.96	0.30 ± 0.18

596

597 The biopolymer blend films presented intermediate barrier properties in
 598 comparison to the films made of the neat biopolymers. The PHBV/PLA/PBAT
 599 1:1:1 blend film processed with low-functionality ESAO showed slightly higher
 600 WVP and LP values than the uncompatibilized blend film, but a significantly
 601 lower OP value. As supported above during the morphology analysis, low-
 602 functionality ESAO induced a reduction of both the inclusion phase size and
 603 interface of the biopolymer regions in the blend, which could favor plasticization

604 by water and/or limonene vapors. Alternatively, since oxygen is a
605 noncondensable small permeant, the presence of the newly formed PHBV-*b*-
606 PLA-*b*-PBAT terpolymer may also reduce the free volume of the ternary blend
607 and, then, lower diffusion of the oxygen molecules. A previous work performed
608 on the barrier properties of biopolymer blends has reported that
609 PLA/poly(propylene carbonate) (PPC) cast films processed with 0.5 phr multi-
610 functional ESAO exhibited optimum performance and certain compatibility, but
611 it did not experience any positive influence on the WVP and OP compared to
612 their corresponding uncompatibilized binary blend.^[47] In general, increasing the
613 content of PHBV in the biopolymer blends increased the barrier performance to
614 both water vapor and oxygen, whereas it decreased the limonene barrier
615 properties. In particular, the PHBV/PLA/PBAT 3:1:1 compatibilized by low-
616 functionality ESAO showed the most balanced barrier performance. This
617 biopolymer blend film presented a WVP value similar to that of compression-
618 molded films of petroleum-derived PET, *i.e.* $2.30 \times 10^{-15} \text{ kg m m}^{-2} \cdot \text{Pa}^{-1} \text{ s}^{-1}$, but
619 with considerably lower LP and OP values, *i.e.* $1.17 \times 10^{-13} \text{ kg m m}^{-2} \cdot \text{Pa}^{-1} \text{ s}^{-1}$ and
620 $1.35 \times 10^{-19} \text{ m}^3 \text{ m m}^{-2} \cdot \text{Pa}^{-1} \text{ s}^{-1}$, respectively.^[60,61] Therefore, a potential application
621 of the here-developed biopolymer ternary blends in medium and medium-to-
622 high barrier packaging applications are foreseen.

623 **4. CONCLUSIONS**

624 The present study describes the preparation and characterization of novel
625 biopolymer ternary blends made of PHBV, PLA, and PBAT. The neat PHBV film,
626 which was the major component of the blends, presented poor thermal stability,
627 extremely low ductility, and low barrier to limonene (aroma) but high
628 crystallinity, sufficient mechanical strength, and good barrier properties to water
629 and oxygen. The incorporation of PLA improved both processability and aroma
630 barrier while PBAT offered higher ductility and slightly better thermal stability.
631 The resultant uncompatibilized biopolymer blends then showed an intermediate
632 mechanical and barrier performance, however these were immiscible and still
633 presented a relatively low thermal stability and poor ductility.

634 The addition of low-functionality ESAO successfully increased the miscibility of
635 the blended biopolymers, acting as a reactive compatibilizer during melt
636 compounding. After the achievement of partial compatibilization, the coarse
637 morphology of the soften inclusion phase in the immiscible blend changed to a
638 finer morphology, inducing a more ductile fracture behavior. Though the effect
639 of low-functionality ESAO on the thermal stability of the biopolymer blends was
640 low, this reactive additive provided enhanced overall mechanical performance,
641 particularly in terms of elongation at break, as well as higher oxygen barrier. This
642 enhancement was proposed to be achieved by the *in situ* formation of a newly
643 linear PHBV-*b*-PLA-*b*-PBAT terpolymer and the copolymers of thereof, which
644 were produced at the biopolymers interface due to reaction between the multiple
645 epoxy groups of ESAO with the functional terminal groups of the biopolymers.
646 Due to the inherent low functionality of ESAO and the more favorable reactivity
647 of the epoxy groups with the carboxyl groups in polyesters, the reaction mainly
648 produced a linear connection of the biopolymer chains, avoiding the formation
649 of highly branched and/or cross-linked structures and facilitating the
650 processability of the films.

651 Finally, the here-prepared biopolymer ternary blends presented tunable
652 properties, depending on the selected mixing ratio. The ternary blends with high

653 contents of PHBV share some similarities with traditional rigid polymers such as
654 PET, PS, and PC, which makes them attractive as a sustainable alternative in the
655 food packaging field for disposable and compostable articles. These biopolymer
656 articles can find potential uses as packaging materials requiring moderate barrier
657 performance such as, among others, food trays and lids.

658 ACKNOWLEDGEMENTS

659 This research was funded by the EU H2020 project YPACK (reference number
660 773872) and by the Spanish Ministry of Economy and Competitiveness
661 (MINECO) with project numbers MAT2017-84909-C2-2-R and AGL2015-63855-
662 C2-1-R. L. Quiles-Carrillo wants to thank the Spanish Ministry of Education,
663 Culture, and Sports (MECD) for financial support through his FPU grant number
664 FPU15/03812.

665 REFERENCES

- 666 [1] R. P. Babu, K. O'Connor, R. Seeram, *Progress in Biomaterials* **2013**, 2, 8.
667 [2] S. Torres-Giner, A. Torres, M. Ferrándiz, V. Fombuena, R. Balart, *Journal of Food Safety*
668 **2017**, 37, e12348.
669 [3] L. Quiles-Carrillo, N. Montanes, T. Boronat, R. Balart, S. Torres-Giner, *Polymer Testing*
670 **2017**, 61, 421.
671 [4] A. Steinbüchel, H. E. Valentin, *FEMS Microbiology Letters* **1995**, 128, 219.
672 [5] C. W. J. McChalicher, F. Srienc, *Journal of Biotechnology* **2007**, 132, 296.
673 [6] K. C. Reis, J. Pereira, A. C. Smith, C. W. P. Carvalho, N. Wellner, I. Yakimets, *Journal*
674 *of Food Engineering* **2008**, 89, 361.
675 [7] E. T. H. Vink, S. Davies, *Industrial Biotechnology* **2015**, 11, 167.
676 [8] R. P. John, K. M. Nampoothiri, A. Pandey, *Process Biochemistry* **2006**, 41, 759.
677 [9] K. Madhavan Nampoothiri, N. R. Nair, R. P. John, *Bioresource Technology* **2010**, 101,
678 8493.
679 [10] D. Garlotta, *Journal of Polymers and the Environment* **2001**, 9, 63.
680 [11] L. T. Lim, R. Auras, M. Rubino, *Progress in Polymer Science* **2008**, 33, 820.
681 [12] L. Quiles-Carrillo, N. Montanes, C. Sammon, R. Balart, S. Torres-Giner, *Industrial*
682 *Crops and Products* **2018**, 111, 878.
683 [13] L. Quiles-Carrillo, M. M. Blanes-Martínez, N. Montanes, O. Fenollar, S. Torres-
684 Giner, R. Balart, *European Polymer Journal* **2018**, 98, 402.
685 [14] L. Quiles-Carrillo, S. Duarte, N. Montanes, S. Torres-Giner, R. Balart, *Materials &*
686 *Design* **2018**, 140, 54.

- 687 [15] U. Witt, R.-J. Müller, W.-D. Deckwer, *Journal of environmental polymer degradation*
688 **1997**, 5, 81.
- 689 [16] K. O. Siegenthaler, A. Künkel, G. Skupin, M. Yamamoto, "Ecoflex® and Ecovio®:
690 Biodegradable, Performance-Enabling Plastics", in *Synthetic Biodegradable Polymers*, B.
691 Rieger, A. Künkel, G.W. Coates, R. Reichardt, E. Dinjus, and T.A. Zevaco, Eds., Springer
692 Berlin Heidelberg, Berlin, Heidelberg, 2012, p. 91.
- 693 [17] L. Jiang, M. P. Wolcott, J. Zhang, *Biomacromolecules* **2006**, 7, 199.
- 694 [18] R. P. H. Brandelero, F. Yamashita, M. V. E. Grossmann, *Carbohydrate Polymers* **2010**,
695 82, 1102.
- 696 [19] R. Muthuraj, M. Misra, A. K. Mohanty, *Journal of Polymers and the Environment* **2014**,
697 22, 336.
- 698 [20] R. S. Porter, L.-H. Wang, *Polymer* **1992**, 33, 2019.
- 699 [21] C. Koning, M. Van Duin, C. Pagnoulle, R. Jerome, *Progress in Polymer Science* **1998**,
700 23, 707.
- 701 [22] R. Muthuraj, M. Misra, A. K. Mohanty, *Journal of Applied Polymer Science* **2017**, 45726.
- 702 [23] A. J. Ryan, *Nature Materials* **2002**, 1, 8.
- 703 [24] D. Wu, Y. Zhang, L. Yuan, M. Zhang, W. Zhou, *Journal of Polymer Science Part B:*
704 *Polymer Physics* **2010**, 48, 756.
- 705 [25] C. H. Kim, K. Y. Cho, E. J. Choi, J. K. Park, *Journal of Applied Polymer Science* **2000**, 77,
706 226.
- 707 [26] R. Supthanyakul, N. Kaabbuathong, S. Chirachanchai, *Polymer* **2016**, 105, 1.
- 708 [27] Y.-H. Na, Y. He, X. Shuai, Y. Kikkawa, Y. Doi, Y. Inoue, *Biomacromolecules* **2002**, 3,
709 1179.
- 710 [28] J.-B. Zeng, K.-A. Li, A.-K. Du, *RSC Advances* **2015**, 5, 32546.
- 711 [29] M. Xanthos, S. S. Dagli, *Polymer Engineering & Science* **1991**, 31, 929.
- 712 [30] U. Sundararaj, C. W. Macosko, *Macromolecules* **1995**, 28, 2647.
- 713 [31] S. T. Milner, H. Xi, *Journal of Rheology* **1996**, 40, 663.
- 714 [32] M. Villalobos, A. Awojulu, T. Greeley, G. Turco, G. Deeter, *Energy* **2006**, 31, 3227.
- 715 [33] S. Torres-Giner, N. Montanes, T. Boronat, L. Quiles-Carrillo, R. Balart, *European*
716 *Polymer Journal* **2016**, 84, 693.
- 717 [34] H. J. Lehermeier, J. R. Dorgan, *Polymer Engineering & Science* **2001**, 41, 2172.
- 718 [35] B. Liu, Q. Xu, *Journal of Materials Science and Chemical Engineering* **2013**, 1, 9.
- 719 [36] H. Eslami, M. R. Kamal, *Journal of Applied Polymer Science* **2013**, 129, 2418.
- 720 [37] T. Loontjens, K. Pauwels, F. Derks, M. Neilen, C. K. Sham, M. Serné, *Journal of Applied*
721 *Polymer Science* **1997**, 65, 1813.
- 722 [38] V. Ojijo, S. S. Ray, *Polymer* **2015**, 80, 1.
- 723 [39] V. Frenz, D. Scherzer, M. Villalobos, A. A. Awojulu, M. Edison, R. Van Der Meer,
724 "Multifunctional polymers as chain extenders and compatibilizers for polycondensates
725 and biopolymers", in *Technical Papers, Regional Technical Conference - Society of Plastics*
726 *Engineers*, 2008, p. 3/1678.
- 727 [40] L. A. Utracki, *The Canadian Journal of Chemical Engineering* **2002**, 80, 1008.
- 728 [41] R. Al-Ittry, K. Lamnawar, A. Maazouz, *Polymer Degradation and Stability* **2012**, 97,
729 1898.
- 730 [42] S. Lin, W. Guo, C. Chen, J. Ma, B. Wang, *Materials & Design (1980-2015)* **2012**, 36, 604.
- 731 [43] L. C. Arruda, M. Magaton, R. E. S. Bretas, M. M. Ueki, *Polymer Testing* **2015**, 43, 27.

732 [44] Y. Wang, C. Fu, Y. Luo, C. Ruan, Y. Zhang, Y. Fu, *Journal Wuhan University of*
733 *Technology, Materials Science Edition* **2010**, 25, 774.

734 [45] D. Wei, H. Wang, H. Xiao, A. Zheng, Y. Yang, *Carbohydrate Polymers* **2015**, 123, 275.

735 [46] M. A. Abdelwahab, S. Taylor, M. Misra, A. K. Mohanty, *Macromolecular Materials and*
736 *Engineering* **2015**, 300, 299.

737 [47] Q. Sun, T. Mekonnen, M. Misra, A. K. Mohanty, *Journal of Polymers and the*
738 *Environment* **2016**, 24, 23.

739 [48] S. Torres-Giner, J. V. Gimeno-Alcañiz, M. J. Ocio, J. M. Lagaron, *Journal of Applied*
740 *Polymer Science* **2011**, 122, 914.

741 [49] T. Miyata, T. Masuko, *Polymer* **1998**, 39, 5515.

742 [50] R. Muthuraj, M. Misra, A. K. Mohanty, *Journal of Applied Polymer Science* **2015**, 132,
743 n/a.

744 [51] J. Ren, H. Fu, T. Ren, W. Yuan, *Carbohydrate Polymers* **2009**, 77, 576.

745 [52] M. Jamshidian, E. A. Tehrany, M. Imran, M. Jacquot, S. Desobry, *Comprehensive*
746 *Reviews in Food Science and Food Safety* **2010**, 9, 552.

747 [53] L. Savenkova, Z. Gercberga, V. Nikolaeva, A. Dzene, I. Bibers, M. Kalnin, *Process*
748 *Biochemistry* **2000**, 35, 573.

749 [54] A. R. M. Costa, T. G. Almeida, S. M. L. Silva, L. H. Carvalho, E. L. Canedo, *Polymer*
750 *Testing* **2015**, 42, 115.

751 [55] K. Zhang, A. K. Mohanty, M. Misra, *ACS Applied Materials & Interfaces* **2012**, 4, 3091.

752 [56] N. Zhang, Q. Wang, J. Ren, L. Wang, *Journal of Materials Science* **2009**, 44, 250.

753 [57] W. Chinsirikul, J. Rojsatean, B. Hararak, N. Kerddonfag, A. Aontee, K. Jaieau, P.
754 Kumsang, C. Sripethdee, *Packaging Technology and Science* **2015**, 28, 741.

755 [58] R. Auras, B. Harte, S. Selke, *Journal of Applied Polymer Science* **2004**, 92, 1790.

756 [59] M. D. Sanchez-Garcia, E. Gimenez, J. M. Lagaron, *Carbohydrate Polymers* **2008**, 71,
757 235.

758 [60] M. D. Sanchez-Garcia, E. Gimenez, J. M. Lagaron, *Journal of Plastic Film & Sheeting*
759 **2007**, 23, 133.

760 [61] J. M. Lagaron, "Multifunctional and nanoreinforced polymers for food packaging",
761 in *Multifunctional and Nanoreinforced Polymers for Food Packaging*, Woodhead Publishing,
762 Cambridge, UK, 2011, p. 1.

763